Pflugers Arch - Eur J Physiol (2012) 464:317–330
DOI 10.1007/s00424-012-1137-4

SIGNALING AND CELL PHYSIOLOGY

Influence of WNK3 on intracellular chloride concentration and volume regulation in HEK293 cells

Silvia Cruz-Rangel · Gerardo Gamba · Gerardo Ramos-Mandujano · Herminia Pasantes-Morales

Received: 6 June 2012 / Revised: 6 July 2012 / Accepted: 7 July 2012 / Published online: 3 August 2012

Abstract The involvement of WNK3 (with no lysine [K] kinase) in cell volume regulation evoked by anisotonic conditions was investigated in two modified stable lines of HEK293 cells: WNK3+, overexpressing WNK3 and WNK3-KD expressing a kinase inactive by a punctual mutation (D294A) at the catalytic site. This different WNK3 functional expression modified intracellular Cl^- concentration with the following profile: WNK3+>control>WNK3-KD cells. Stimulated with 15 % hypotonic solutions, WNK3 + cells showed less efficient RVD (13.1 %), lower Cl^- efflux and decreased (94.5 %) KCC activity. WNK3-KD cells showed 30.1 % more efficient RVD, larger Cl^- efflux and 5-fold higher KCC activity, increased since the isotonic condition. Volume-sensitive Cl^- currents were similar in controls, WNK3+ cells, and WNK3-KD cells. Taurine efflux was not evoked at H15%. These results show a WNK3 influence on RVD in HEK293 cells via increasing KCC activity. Hypertonic medium induced cell shrinkage and RVI. In both WNK3+ and WNK3-KD cells, RVI and NKCC activity were increased, in WNK3+ cells presumably by enhanced NKCC phosphorylation, and in WNK3-KD cells via the $[Cl^-]_i$ reduction induced by the higher KCC activity in characteristic of these cells. These results support the role of WNK3 in modulation of intracellular Cl^- concentration, in RVD, and indirectly on RVI, via its effects on KCC and NKCC activity. WNK3 in HEK293 cells is expressed as *puncta* at the intercellular junctions and diffusely at the cytosol, while the inactive kinase was found concentrated at the Golgi area. Cells with inactive WNK3 exhibited a marked change of cell phenotype.

Keywords RVI · RVD · NKCC · KCC · Osmolarity · Kinase · SPAK

S. Cruz-Rangel · G. Ramos-Mandujano · H. Pasantes-Morales (✉)
División de Neurociencias, Instituto de Fisiología Celular, Universidad Nacional Autónoma de México, Ciudad Universitaria, Circuito Exterior, 04510 Mexico, DF, Mexico
e-mail: hpasante@ifc.unam.mx

G. Gamba
Departamento de Medicina Genómica, Instituto de Investigaciones Biomédicas, Universidad Nacional Autónoma de México, Mexico City, Mexico

G. Gamba
Departamento de Nefrología y Metabolismo Mineral, Instituto Nacional de Ciencias Médicas y Nutrición Salvador Zubirán, Mexico City, Mexico

Introduction

Each cell lineage has a characteristic volume that is maintained within narrow ranges of variation along the cell life. This ability to maintain a constant volume is present in most cell types and has been preserved through evolution. In terrestrial species, the osmolarity of the external milieu is strictly regulated and most cells are not exposed to changes in external osmolarity. Exceptions are intestinal cells and some cells from the renal system, which are physiologically exposed to broad variations in osmolarity. Adaptive mechanisms for cell volume regulation facing a variation in external osmolarity are based on increasing water fluxes in the necessary direction to restore the osmotic equilibrium. The cell decrease facing hypotonic swelling is known as regulatory volume decrease (RVD), and the cell volume gain after hypertonic shrinkage is the regulatory volume increase (RVI). Volume regulation is an active process which occurs even if the external anisotonic condition persists, and is achieved in most cases by translocation of osmotically active solutes between the extracellular and intracellular compartments, modifying the water potential.

Osmolytes involved are those present in concentrations sufficiently high as to make a significant contribution to water potential. The ions Na^+, K^+, and Cl^-, and the organic osmolytes. Amino acids, polyalcohols, urea, and creatinine, are the main osmolytes involved in volume regulation, Na^+ and Cl^- for RVI and K^+ and Cl^- for RVD. Cotransporters or/and channels accomplish the osmolyte translocation [14, 31].

The electroneutral *cation–chloride coupled* cotransporters (SLC12A family) involved in volume regulation are the NCC and NKCC1/2 for RVI and KCCs for RVD [9, 42]. Volume-responsive K^+ and Cl^- channels also participate, particularly during RVD. Organic osmolytes are translocated by Na^+-dependent cotransporters during RVI and by diffusion pathways in RVD [14, 34, 35]. Cell volume sensors and the signaling chains activating the regulatory cotransporters are poorly known. It has been proposed that WNKs may be part of these transduction mechanisms [32]. WNKs are a family of serine–threonine protein kinases widely distributed in mammalian cells and tissues, regulating the activity of ion channels and cotransporters [19, 26, 46]. Four members of the WNK family, WNK1–4, have been identified [18, 19]. WNK1 and WNK4 are responsive to hypertonicity [23, 43, 46, 47] and regulate the activity of the ion cotransporters [18, 19, 46]. WNK1 increases NKCC1 activity [1] and WNK4 decreases the activity of KCCs [8, 10]. WNK3 is of particular interest because it reciprocally regulates the activity of both NKCCs and KCCs. In the heterologous expression system of *Xenopus laevis* oocytes, WNK3 activates NKCC1, NKCC2, and NCC and inactivates the KCCs [5, 18, 37, 39]. The catalytically inactive version of WNK3 obtained by substitution of the aspartate 294 for alanine (WNK3-D294A) does the opposite: inhibition of NKCCs and activation of KCCs under isotonic conditions, with lower activation by changes in external osmolarity [32]. The known contribution of these transporters on volume regulation, prompted us to investigate the influence of WNK3 on RVD and RVI in a mammalian cell system, the embryonic renal cell line HEK293. For this purpose, two stable transformed cell lines were created that either overexpress the wild-type WNK3 or a catalytically inactive form, the WNK3-D294A. The activity of KCC, the volume-sensitive Cl^- currents, the intracellular Cl^- levels, and RVD were examined in the two cell lines. NKCC1 activity and RVI were also investigated. The cell localization and translocation of WNK3 in response to changes in cell volume were examined.

Materials and methods

Stable cell lines and cell culture

The full-length human WNK3 cDNA was subcloned into the mammalian expression vector pcDNA3.1/NT-GFP TOPO (Invitrogen) with 5′ KpnI and 3′ NotI restriction sites. WNK3 was fused in frame to the 3′ end of the GFP. Site-directed mutagenesis was performed on WNK3 cDNA to generate kinase dead WNK3-KD using the QuikChange Mutagenesis kit (Stratagene). All constructs were verified by automatic DNA sequencing. To generate the stable cell lines, HEK293 cells grown on 35-mm diameter dishes (90 % confluence) were transfected with 1 μg of each construct (pCDNA-WNK3, pCDNA-WNK3-KD, or empty vector) using Lipofectamine 2000® (Invitrogen) according the manufacturer's protocol. After 24 h, transfected cells were selected in a medium supplemented with 3 mg/ml G418 (Calbiochem, Merck Millipore), and the culture medium was replaced every 36 h maintaining the antibiotic. After 2 weeks, fluorescent single clones were isolated and subcultured in selection media (1 mg/ml G418). The presence of the endogenous and overexpressed WNK3-GFP protein was detected by immunobloting assay.

HEK293, empty vector (V), overexpressing WNK3 (WNK3+), and WNK3-KD cell lines were maintained in Dulbecco's Modified Eagle Medium supplemented with 10 % FBS, 50 U/ml penicillin, and 50 μg/ml streptomycin (all from GIBCO), in a humidified atmosphere containing 5 % CO_2 and 95 % air at 37 °C. Cells were plated on 35-mm dishes at 1.5×10^5 cells/dish for ^{3}H-taurine release and Rubidium-86 (^{86}Rb) uptake (American Radiolabeled Chemicals and PerkinElmer, respectively), and at 25×10^3 cells/dish for intracellular Cl^- assays and for electrophysiological recordings. Cells were used after 2–3 days of plating.

Western blot analysis

For immunoblotting assays, cells cultured on 60-mm dishes were washed, and then scraped into lysis buffer containing 20 mM Tris/HCl pH 7.4, 1 mM EDTA, 50 mM NaCl, 1 mM EGTA, 1 % Triton X-100, 0.5 mM Na_3VO_4, and 1 mM 2-glycerophosphate. Cell homogenates were sonicated and clarified by centrifugation for 5 min at 11,000×*g* and protein concentration determined by the Bradford method. Then, 80 μg of protein was separated by SDS-PAGE (7.5 % acrylamide gel) and transferred onto PVDF membranes (Bio-Rad). Membranes were blocked with TBS-T (Tris-buffered saline/Tween 20; 100 mM Tris/HCl, 150 mM NaCl, and 0.1 % Tween 20, pH 7.5) containing 5 % (*w/v*) non-fat dried milk and incubated (1:1,000) overnight at 4 °C, with the rabbit primary antibodies anti-WNK3 (Alpha Diagnostic International), anti-GFP or anti-β actin (Santa Cruz Biotechnology). After further washing, blots were incubated with HRP-conjugated goat anti-rabbit IgG antibody (1:7,500; Zymed) for 1 h at room temperature. Chemoluminiscent reaction was assayed using ECL®-Plus Western Blot Detection Reagents (GE Healthcare) according to the manufacturer's recommendations, and bands were visualized with exposition to Kodak BioMax light films (Sigma).

Immunocytochemistry

Cells cultured on round cover glasses (25×10^3 cells in 35-mm dishes) were fixed with 4 % paraformaldehyde (15 min), washed (three times, 5 min each) with PBS+0.1 % BSA, permeabilized/blocked with PBS+0.1 % BSA+10 % goat serum+0.3 % Triton 100×, during 1 h, at room temperature. Cover glasses were incubated with the antibodies rabbit anti-WNK3 (1:100, Alpha Diagnostic International), mouse anti-occludin (1:100, Zymed), or mouse anti-golgin-97 (1:60, Molecular Probes) overnight at 4 °C. After incubation, cells were washed and incubated with the secondary antibodies FITC conjugated goat anti-rabbit IgG (1:250, Zymed) or CY5-conjugated goat anti-mouse IgG (1:250, Molecular Probes) at room temperature for 1 h and washed. The coverslips were mounted on glass slides containing 20 µl Vectashield mounting medium with DAPI (Vector Laboratories). Microphotographs were obtained on a confocal microscope (Olympus FluoView FV1000).

Measurement of changes in cell volume

Cell volume changes in the experimental conditions were measured as the cell volume decrease or increase relative to volume in isotonic conditions. Isotonic medium contained (in mM): 160 NaCl, 5 KCl, 1.17 $MgSO_4$, 1 $CaCl_2$, 10 glucose, and 10 HEPES, pH 7.4, with an osmolarity of 350 mOsm. The composition of this medium was made to match the osmolarity of the culture medium (345±5 mOsm) in which the cells are grown. Osmolarities of media and solutions were determined with a freezing point osmometer (Osmette A, Precision Systems Inc, Natick, MA). Volume measurements were carried out using a large angle light scattering system according to [36]. Cells were cultured on rectangular cover glasses (10×50 mm) at 90 % confluence at the time of experiments. Cover glasses were placed at a 50° angle relative to the incident light in a cuvette with 1 ml of isotonic medium in a Fluoromax-3 Horiba luminescence spectrometer. Cells were excited at 585 nm with an argon arc lamp and light scattering was detected at the same wavelength. Cells were maintained during 100 s in isotonic solution (2 ml). The hypotonic solution (298 mOsm) was obtained by adding to the cuvette 1 ml of a solution containing the reduced NaCl concentration required to reach 298 mOsm, i.e., 15 % hypotonic. The hypertonic (600 mOsm) solution was obtained by addition to the cuvette of 1 ml of the isotonic medium plus 500 mM sorbitol, to reach a final osmolarity of 600 mOsm. Results are expressed as the inverse of the emission signal as light intensity inversely correlates with cell volume, according to the equation I_o/I_t (where I_o is the emission signal average when basal signal has been reached just before the stimulus; I_t is the emission signal at time t).

Electrophysiological recordings and data analysis

Electrophysiological recording was carried out on cells seeded on 35-mm dishes. Currents were measured with an Axopatch 200 patch-clamp amplifier (Axon Instruments, Molecular Devices, Ontario, Canada) using the whole-cell patch clamp configuration. All recordings were performed at room temperature (25 °C). Patch electrodes were prepared from 1.5-mm OD, 1.0-mm ID borosilicate glass (World Precision Instruments, FL, USA), and had resistances between 3 and 5 MΩ when filled with the pipette solution. The recorded signal was filtered at 10 kHz with a low-pass Bessel filter and transferred to a computer with the Digidata 1200 interface (Axon Instruments). All recordings were acquired and analyzed with pCLAMP6 software (Axon Instruments). Whole-cell currents were elicited by 300 ms duration voltage steps ranging from −100 to +100 mV in 20 mV increments, from a holding potential of 0 mV. The voltage protocol was carried out every 2 min and the current at 100 mV monitored to insure steady-state recordings. To express currents as current densities, the capacitance of the cell was measured at the beginning of the whole-cell recording by integrating the capacitive current transient. The standard pipette solution contained (in mM): 117.5 CsCl, 20 TEA-Cl, 1 $MgCl_2$, 10 HEPES, 1 EGTA, 0.7 $CaCl_2$ (approximately 200 nM buffered calcium), 44 mannitol, and 5 Mg ATP, pH 7.4 and 335 mOsm. The bath solution had the following composition (in mM): 135 NaCl, 5 KCl, 1.7 $MgSO_4$, 1 $CaCl_2$, 5 glucose, 10 HEPES, 50 mannitol, pH 7.4, and 350 mOsm. The hypotonic bath solution (298 mOsm) was prepared by omitting mannitol from the standard bath solution. This procedure did not alter the Cl^- reversal potential (0 mV). Solution changes were carried out using a peristaltic pump-based perfusion system. For experiments with blockers, DCPIB (10 µM; Tocris Bioscience) or DIOA (20 µM) (Sigma) were added in hypotonic medium after the volume-sensitive currents were developed.

Na^+–K^+–$2Cl^-$ and K^+–Cl^- cotransporters activity

Bumetanide-sensitive ^{86}Rb uptake assays were used to measure the activity of the Na^+–K^+–$2Cl^-$ cotransporter in hypotonic (298 mOsm) or hypertonic (600 mOsm) conditions. Cells were pre-incubated for 30 min in a Cl^--free medium (in mM: 150 Na^+ gluconate, 10 K^+ gluconate, 4.6 Ca^{2+} gluconate, 1 $MgSO_4$, 5 glucose, and 10 HEPES/Tris, pH 7.4) containing 0.1 mM ouabain (Sigma) and then transferred to the uptake medium (in mM: 160 NaCl, 10 KCl, 1 $CaCl_2$, 1 $MgSO_4$, 5 glucose, and 5 HEPES/Tris, pH 7.4) containing 0.1 mM ouabain plus 1 µCi ^{86}Rb/ml for 3 or 15 min. ^{86}Rb uptake due only to NKCC activity was calculated by subtraction of the uptake in the presence of 10 µM bumetanide (Sigma).

K^+–Cl^- cotransport was assessed by measuring Cl^--dependent ^{86}Rb uptake under isotonic or hypotonic conditions (350 and 298 mOsm). Cells were pre-incubated in a Na^+-free, Cl^--free medium (in mM: 150 *N*-methyl-D-glucamine gluconate, 10 K^+ gluconate, 4.6 Ca^{2+} gluconate, 1 $MgSO_4$, 5 glucose, and 5 HEPES/Tris, pH 7.4) containing 0.1 mM ouabain, during 30 min. Cells were then transferred to a Na^+-free medium (in mM: 150 *N*-methyl-D-glucamine-Cl^-, 10 KCl, 1 $CaCl_2$, 1.7 $MgSO_4$, 5 glucose, and 10 HEPES/Tris, pH 7.4) containing 0.1 mM ouabain and ^{86}Rb 1 μC_i/ml and uptake proceeded during 10 min. The extracellular Na^+ removal prevents ^{86}Rb uptake by the endogenous NKCC cotransporter. The Cl^--dependent ^{86}Rb uptake due to KCCs was obtained by subtraction of uptake in Cl^--free medium (Cl^- substituted by gluconate).

Determination of changes in intracellular Cl^- by epifluorescence

Changes in intracellular Cl^- were measured using the fluorescent Cl^- ion indicator, 6-methoxy-*N*-ethylquinolinium iodide (MEQ). MEQ was placed under a stream of N_2 adding the reducing agent, sodium borohydride (30 μM) to create the cell-permeable form dihydro-MEQ (diH-MEQ). Cells on 35 mm dishes were incubated during 10 min with freshly prepared diH-MEQ (25 μM). After loading, cells were washed and incubated 15 min at 37 °C to obtain a homogeneous intracellular distribution. The diH-MEQ loaded into cells is rapidly reoxidized to the cell-impermeant, Cl^--sensitive fluorescent MEQ (absorption/emission maximal of 344/440 nm). Fluorescent cells were observed on an epifluorescence microscope Olympus IX71. A peristaltic pump-based perfusion system (1 ml/min) was used to measure the effect of hypotonicity on intracellular Cl^- concentration. Cells were perfused during 5 min with isotonic medium (basal recordings) and then perfused with the hypotonic medium during 15 min. Images of cells were captured every minute using a digital camera, and fluorescence brightness intensities were determined using an Image J software (ImageJ 1.36b NIH, USA). In order to calibrate MEQ fluorescence and estimate intracellular $[Cl^-]_i$ we used the Stern–Volmer equation $F_0/F_{Cl-}=1+K_q\,[Cl^-]_i$. Amphotericin B (10 μM) was added in all solutions to equilibrate intracellular and extracellular Cl^- concentrations. Briefly, cells were placed in a free-Cl^- isotonic medium (140 mM of K^+-gluconate and 4.6 mM of Ca^{2+}-gluconate, pH 7.4) by 5 min. Solutions containing three different Cl^- concentrations (20, 40, and 80 mM) were then sequentially added. Finally, the fluorescence was completely quenched by adding a KSCN 160 mM (background fluorescence). The total quenchable signal (F_0) was calculated by subtracting the fluorescence in the presence of KSCN from the fluorescence in the free-Cl^- medium. The ratio of F_0 to the fluorescence in the presence of increasing $[Cl^-]$ (F_{Cl-}) is given as F_0/F_{Cl-}, where F_{Cl-} is the fluorescence in the presence of a given Cl^- concentration. A plot of F_0/F_{Cl-} versus $[Cl^-]$ provides a slope, from which the Stern–Volmer constant (K_q) is obtained to determine the Cl^- concentration in each experiment [13].

Results

Generation of stable HEK-293 cells lines overexpressing WNK3 and WNK3-KD

Two cell lines were generated to examine the influence of WNK3 on cell volume regulation. One of these exhibits WNK3 overexpression from a cDNA cloned in pcDNA3.1/NT-GFP vector as described in "Materials and methods". This cell line is referred as WNK3+. The second cell line contains a cDNA of the catalytically inactive WNK3-D294A. These cells are referred in this study as WNK3-KD cells (from WNK3-kinase dead). A cell line containing the empty vector (V cell line) was used as control.

WNK3 expression in HEK293 detected by an anti-WNK3 antibody shows two bands in the Western blot. The signal of the upper band is higher in the transfected cells lines (Fig. 1a). This band co-migrates with the transfected pcDNA/GFP-WNK3, detected by the anti-GFP antibody. This confirms the expression of the WNK3 protein in both cell lines (Fig. 1a). Noteworthy, transfection of the catalytically inactive WNK3 (WNK3-KD) induced a remarkable change in the cell shape. Cells look flattened and show elongations and filopodia-like extensions (arrows). This morphology is not present in the wild-type (HEK293 WT) or in WNK3+ cells (Fig. 1b).

Cell localization and redistribution upon anisotonic stress

HEK293 WT cells contain endogenous WNK3 that in isotonic conditions was found localized in *puncta* at the intercellular junctions, and diffusely at the cytosol (Fig. 2a). This location was the same in cells overexpressing the kinase in WNK3+ cells (Fig. 2a, d, upper panel). The WNK3 localized at the cellular junctions partly co-localizes with an anti-occludin antibody (Fig. 2d, upper panel). The expression pattern of the inactive kinase was markedly different from that of WNK3. Localization at the cell junctions was notably lower and the signal was accumulated at the cytosol, at an area near the nucleus, which partly co-localizes with anti-golgin-97 antibody (Fig. 2a, d, lower panel).

Exposure of WNK3+ cells to hypotonic medium decreased WNK3 expression from the junction areas, without an evident increase at the cytosol (Fig. 2b and bars). Hypertonic medium (600 mOsm) also reduced the

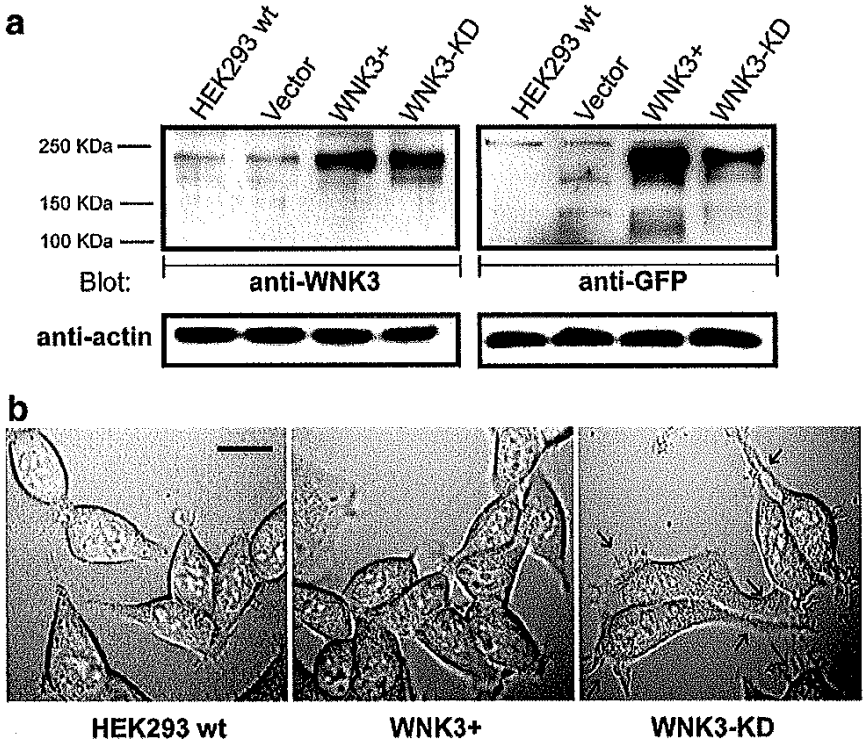

Fig. 1 Expression of WNK3 in wild-type HEK293 (HEK293 WT) cells, in cells overexpressing WNK3 by transfection with cDNA WNK3 (WNK3+) or with the mutated cDNA, catalytically inactive WNK3-KD cells. **a** Stable cell lines were generated as described in "Materials and methods". Cell lysates were separated on a 7.5 % SDS-PAGE gel, transferred to a PVDF membrane, and treated subsequently with anti-WNK3 antibody and anti-GFP antibody. Anti-actin demonstrates equal amounts of loaded protein. Representative blots of three separate determinations. **b** Representative images of the morphology of HEK293 WT, WNK3+, or WNK3-KD cells. *Arrows* indicate the elongations and filopodia-like extensions in WNK3-KD cells. Digital images were obtained in a confocal microscope using differential interference contrast illumination. *Bar* 10 μm

number of *puncta* at the cell junctions and WNK3 now appears more concentrated at the cytosol (Fig. 2c and bars). In WNK3-KD cells, the response to either hypotonic or hypertonic conditions was rather similar, i.e., the kinase prominent expression at the near-nuclear site was reduced and new sites of expression were found at the intercellular junctions (Fig. 2b, c, and bars).

Regulatory volume decrease

Swelling and volume regulation were examined in WNK3+ or in WNK3-KD cells. Cells with the empty vector (V) were used as controls. No significant differences on swelling or cell volume regulation were found between V and non-transfected HEK293 WT cells (Fig. 3a–c). Therefore, V cells were used as controls for most parameters throughout the study. Stimulation of V cells with hypotonic medium (15 % hypotonic solution, made by reducing NaCl; see "Materials and methods") induced the typical fast swelling and RVD pattern. Maximal swelling occurred within 10–20 s, followed by the regulatory process to recover the original cell volume. Two phases were identified in the RVD curves, a fast phase lasting about 2 min after the peak of swelling, and a slow phase through the next 2–15 min (Fig. 3a). RVD efficiency was calculated as the percentage of volume recovery at 15 min, the time of the experiment. In V cells, regulatory volume decrease was of 79.2 % (Fig. 3b).

RVD features were then investigated in WNK3+ and WNK3-KD cells. Figure 3a shows that cell swelling in WNK3+ or WNK3-KD was not significantly different from V cells. RVD at the end of the experiment in WNK3+ cells was mildly reduced (13.1 %), while it was 30.1 % increased in WNK3-KD cells (Fig. 3b). The less efficient RVD in WNK3+ cells was due to a lower rate of the first (2 min) regulatory phase, as shown by the rate constant values shown in Fig. 3c. At this time, RVD in WNK3+ cells is 27.1 % lower than in controls. The increased volume regulation found in WNK3-KD cells is the consequence of an accelerated cell volume decrease in the slow phase (Fig. 3c).

These differences on RVD between control and overexpressed or mutated WNK3, may be ascribed to an effect on one or several of the mechanisms responsible for the volume regulatory process, i.e., KCC, the volume-sensitive Cl^- channel and the organic osmolyte fluxes. The efficiency of these three mechanisms on V, WNK3+, and WNK3-KD cells was then examined. Taurine was selected as representative of organic osmolytes. ^{3}H-taurine release experiments were carried out as previously described [45]. However, in HEK293 cells, no taurine efflux was induced by a 15 % osmolarity decrease, as that used for RVD measurements (% ^{3}H-taurine efflux in 5 min, isotonic 1.24±0.08; hypotonic

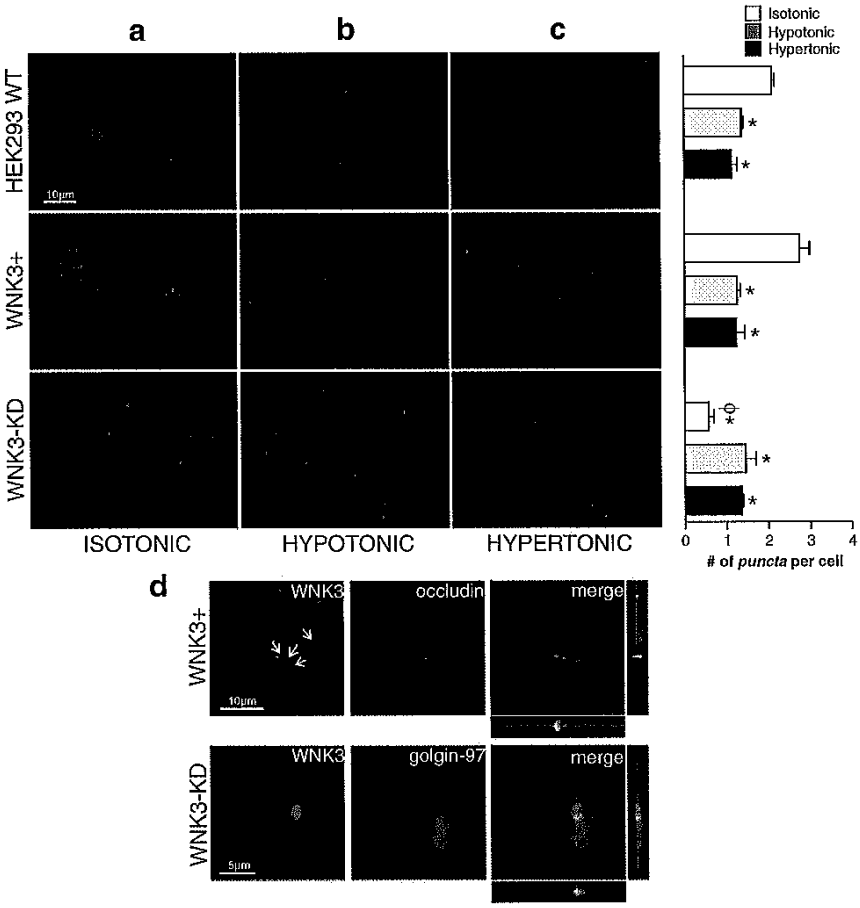

Fig. 2 Expression of WNK3 in HEK293 cells and its relocation by changes in extracellular osmolarity. HEK293 WT, WNK3+, and WNK3-KD cells were left unstimulated (isotonic, **a**) or stimulated with hypotonic (298 mOsm, H15%, **b**) or hypertonic (600 mOsm, **c**) solutions for 3 min, before fixation. *Bars* (means±SE) represent the number of *puncta* per cell, under the different conditions, counted in six images for each condition from different experiments. *Significantly different from isotonic condition in each cell line at $P<0.05$; $^{\Phi}$significantly different from HEK293 WT cells in isotonic condition at $P<0.05$. **d** *Upper panel* WNK3 cells immunostained with anti-WNK3 (*green*), anti-occludin (*magenta pseudocolor*), and merge. *Lower panel* WNK3-KD cells immunostained with anti-WNK3 (*green*), anti-golgin-97 (*red*), and merge. Orthogonal views in merge show the *xy* image plane, *xz* image plane (*bottom*) and *yz* (*right*). Fluorescent imaging was performed using a confocal laser scanning microscope. Representative images of three separate experiments

15 %, 1.28±0.11; 30 % 2.53±0.14; 35 % 4.88±0.36; 40 % 7.06±0.7; $n=4$ for all experiments).

These results suggest that RVD must be supported by the efflux of ion osmolytes, among which Cl^- has a prominent role. WNK3 activity has been suggested to modulate intracellular Cl^- levels $[Cl^-]_i$ via its action on the electroneutral cotransporters [24]. This, though, has not been directly assessed. Changes in $[Cl^-]_i$ in V, WNK3+ and WNK3-KD under basal (isotonic) conditions were first examined.

The Stern–Volmer constant (Kq) in our experimental conditions (medium composition, temperature, and pH) was first determined from a calibration curve at Cl^- concentrations in the range of 0–80 mM (Fig. 4a). The obtained value of 32.3 M^{-1} was used to determine $[Cl^-]_i$ in isotonic medium for V, WNK3+, and WNK3-KD cells. Small but significant differences were found between WNK3+ and WNK3-KD cells, with respect to control V cells. Values found were, in mM, 34.2 (±1.8), 41.6 (±2.4), and 26.4 (±1.4) for V, WNK3+, and WNK3-KD cells, respectively (table, Fig. 4a). These results show that the stable overexpression of functional WNK3 in cells, significantly modifies $[Cl^-]_i$ in the expected direction, that is, wild-type WNK3 increases, whereas mutant WNK3-KD decreases $[Cl^-]_i$, consistent with their effects on the electroneutral cation coupled cotransporters. The hypotonic stimulus (H15%) induced a rapid decline of 24–28 % in $[Cl^-]_i$ in all cells, during the first 4 min, likely due to dilution by water influx. A second phase of gradual reduction in $[Cl^-]_i$ was next observed, attributable to the Cl^- efflux during RVD. Figure 4b shows that $[Cl^-]_i$ reduction, indicative of Cl^- efflux, was significantly lower in WNK3+ cells (12.1 %) and higher in WNK3-KD cells (23.9 %) as compared to control V cells (19.8 %). These values were calculated considering as 100 % the F_0/F_{Cl-} after the dilution phase (min 4).

This Cl^- efflux might be carried either by the activation of volume-sensitive Cl^- channels (ICl^-_{swell}) or/and by the electroneutral cotransporter KCC. Cl^- currents (ICl^-_{swell}) were first examined in all cell lines, using the whole-cell configuration of the patch-clamp technique, as described in "Materials and methods". To focus on the Cl^- currents, we used 73 mM CsCl and 20 mM TEA–Cl in the patch pipette

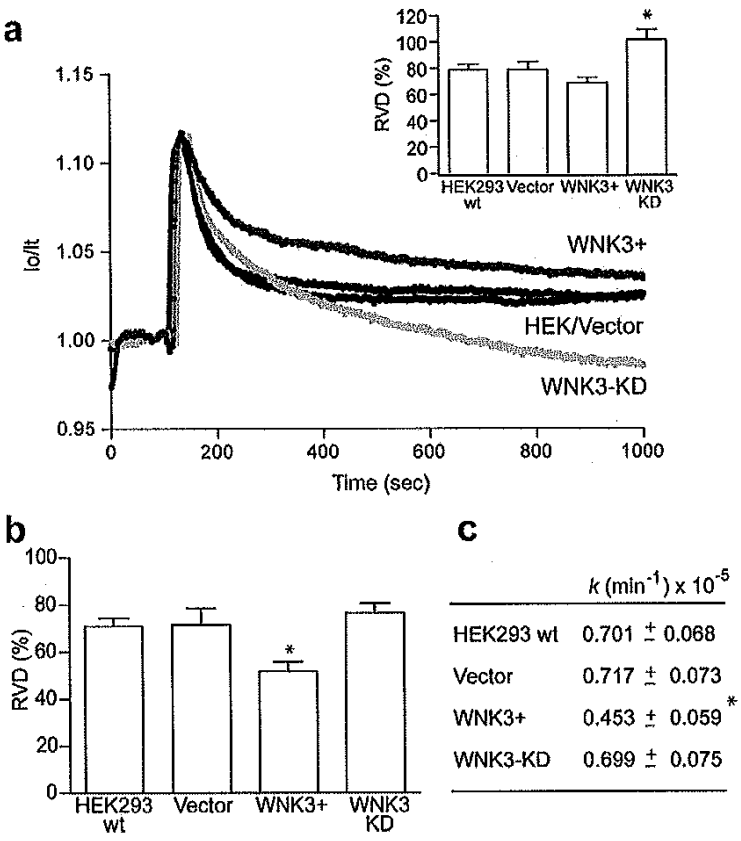

Fig. 3 Swelling and regulatory volume decrease (RVD) in wild-type HEK293, V, WNK3+, or WNK3-KD cells. Changes in cell volume were measured using a large-angle light-scattering system as described in "Materials and methods". **a** Representative traces of changes in cell volume after exposure to 15 % hypotonic (H15%) medium in each cell type. RVD curves are biphasic showing a fast component between 110–200 s and a slow component thereafter. *Bars* (**a**, *inset*) represent the cell volume recovery at the end of the experiment, expressed as percentage of maximal swelling. **b** RVD at the first component. **c** Rate constants from the slope calculated by fitting a linear regression to the logarithmically transformed data during the first 100 s after maximal swelling. Results are means±SE of 15–20 experiments.*Significantly different from control V cells at $P<0.05$

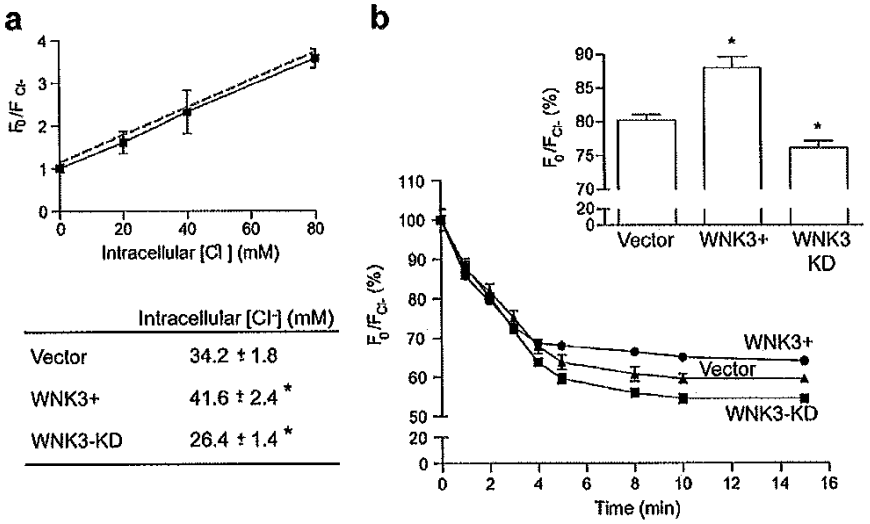

Fig. 4 Changes in intracellular chloride concentration $[Cl^-]_i$ in V, WNK3+, and WNK3-KD cells exposed to hypotonic (H15%) medium. Cells were loaded with diH-MEQ (25 μM) for 10 min as described in "Materials and methods". **a** Calibration plot used to calculate the Stern–Volmer constant (Kq) of 32.3 M^{-1} (regression line, *dotted line*, $r^2=0.99$). **b** Relative reduction of $[Cl^-]_i$ after hypotonic stimulus as percentage of control in isotonic condition for each cell type. For simplicity in the graph, curves show only selected points, from measurements made every minute (**b**, *inset*). *Bars* represent the decrease (%) of $[Cl^-]_i$ from 4–15 min. Mean of three experiments±SEM. *Significantly different from V cells at $P<0.05$

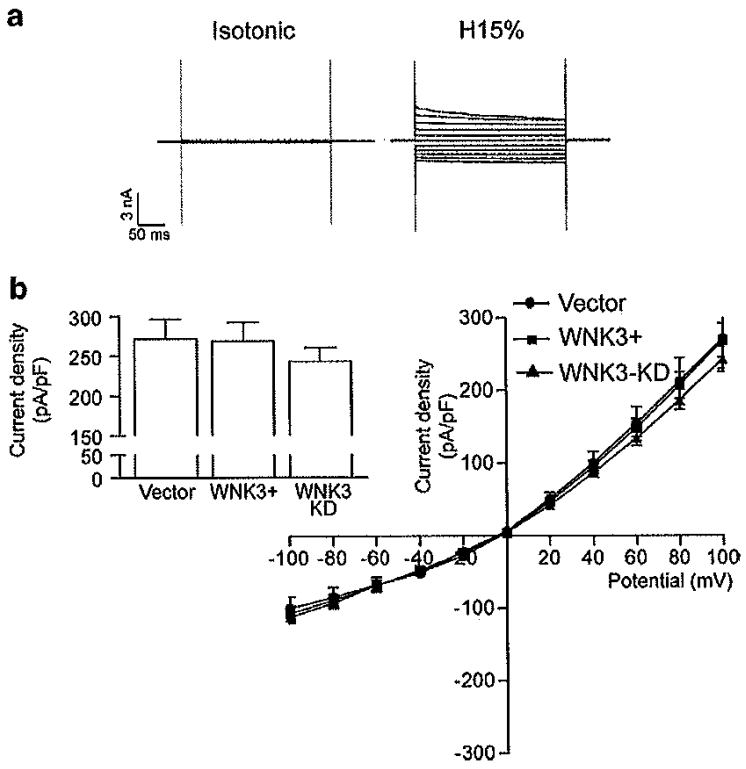

Fig. 5 Whole-cell Cl^- currents activated by hypotonicity in V, WNK3+, and WNK3-KD cells. The holding potential was 0 mV. Currents were elicited by application of step pulses from −100 to +100 mV in 20 mV increments, during 300 ms. a Representative whole-cell current traces at the indicated experimental conditions. The figure shows currents obtained after a 10 min equilibration in the indicated solution. b Current density (pA/pF) vs voltage (mV) curves for V (*circle*), WNK3+ (*square*), and WNK3-KD (*triangle*) cells in hypotonic H15% medium. *Bars* represent the current density of each cell type at +100 mV. Results are means±SE of 7–15 experiments. Values were not significantly different at $P<0.05$

to minimize the contribution of K^+ currents. After obtaining the whole-cell configuration, the isotonic medium was replaced by a 15 % hypotonic solution and evoked currents were registered during 15 min. Upon exposure to hyposmolar conditions, in all cells (V, WNK3+, and WNK3-KD cells) a large current was developed which exhibits the reported features characteristic of ICl^-_{swell} [29]. It is an outwardly rectifying current, with inactivation kinetics at large positive voltages and a reversal potential of −3 mV, close to the reversal equilibrium potential of Cl^- predicted by our solutions of ~0.0 mV (Fig. 5a, b). The membrane current was normalized to the cell membrane capacitance (current density) to correct for different cell sizes. The current density activated by H15% at +100 mV was similar in V and WNK3+ cells (271.1±41.6 pA/pF and 268.7±23.4 pA/pF, respectively), and slightly lower in WNK3-KD cells (242.8±8.6 pA/pF; Fig. 5b).

The KCC activity was measured as the Cl^--sensitive intracellular accumulation of ^{86}Rb (see "Materials and methods") under isotonic or 15 % hypotonic conditions. Basal Cl^--sensitive ^{86}Rb uptake in control V cells was about 8 pmol/(μg protein×min), and this uptake was increased by hypotonicity, raising ^{86}Rb accumulation by almost 2-fold (180 %; Fig.6). In WNK3+ cells both basal and stimulated ^{86}Rb uptake were essentially abolished. Noteworthy, in WNK3-KD cells, ^{86}Rb uptake was already extremely high in isotonic conditions, about 5-fold higher than uptake in V cells, and this was not further increased by hypotonicity (Fig. 6).

To evaluate the contribution of the volume-sensitive Cl^- channel and of KCC to RVD in HEK293 cells, attempts were made to reduce the efficiency of these two mechanisms

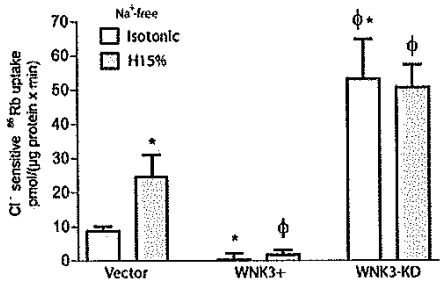

Fig. 6 Effect of hypotonic stimulus on the KCC electroneutral cotransporter activity in control V, WNK3+ or mutant WNK3-KD cells. KCC activity was measured as the Cl^--dependent ^{86}Rb uptake as described in "Materials and methods". KCC activity was measured in isotonic (*clear bar*) or hypotonic H15% (*dark bar*) conditions. Bars represent the mean±SE of 3 separate experiments. *Significantly different from control V cells in isotonic medium at $P<0.01$. ϕ Significantly different from control V cells in H15% at $P<0.05$

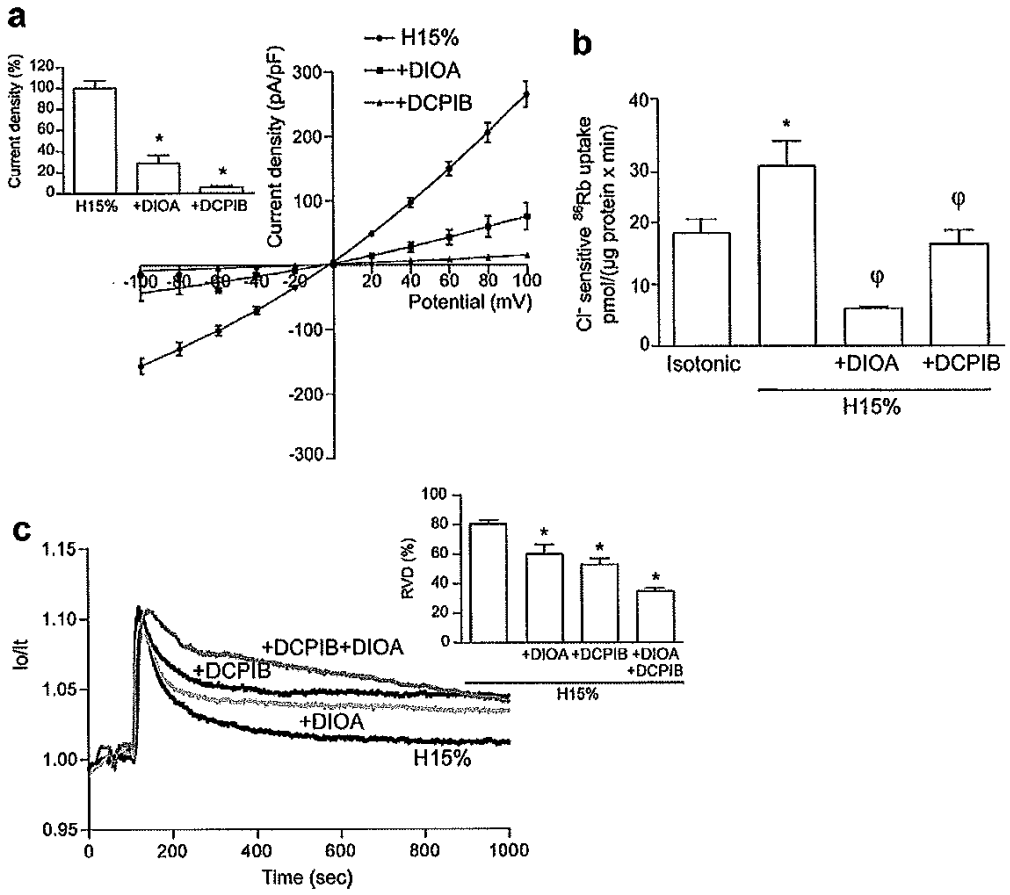

Fig. 7 Effects of DIOA and DCPIB on KCC, ICl^-_{swell}, and RVD in HEK293 cells exposed to H15%. **a** Current density *vs* voltage curves from HEK293 cells in the presence or absence of the blockers ICl^-_{swell} elicited by H15% were recorded as in Fig. 5. The blockers DIOA (20 µM) or DCPIB (10 µM) were added at the time of maximal ICl^-_{swell} current amplitude. Control (*circle*), plus DIOA (*square*), plus DCPIB (*triangle*). *Bars* represent the current density at +100 mV, expressed as 100 % for controls and the corresponding decrease in the presence of the blocker. Results are means±SE of 6–14 experiments. **b** Inhibitory effect of DCPIB and DIOA on the hypotonic-stimulated KCC activity. Cl^--sensitive ^{86}Rb uptake measured as in Fig. 6. Cells were pre-incubated during 30 min with DIOA or DCPIB in isotonic medium before the stimulus and were present throughout the experiment. *Significantly different from the isotonic condition at $P<0.05$; ϕ significantly different from the hypotonic condition at $P<0.05$. **c** RVD after hypotonic (H15%) swelling in HEK293 cells exposed to DIOA, DCPIB, and both. Cells were preincubated with the blockers 30 min before the stimulus and were present throughout the experiment. Results in *bars* (means±SE of 6–16 experiments) represent the cell volume recovery, expressed as percentage of maximal swelling at 300 s after the stimulus. *Significantly different from control H15% at $P<0.05$

by a pharmacological approach. This could not be properly achieved, however, since the two agents commonly used to block KCC (DIOA) or Cl^-_{swell} channel (DCPIB), exerted a potent inhibition on both the cotransporter and the channel. DIOA 20 µM, had a strong inhibitory effect (71.5 %) on the H15%-stimulated Cl^- currents (Fig. 7a), and at the same concentration also reduced (79.3 %) the hypotonic KCC activity (Fig. 7b). Similarly, DCPIB (10 µM) prevented the H15%-stimulated Cl^- currents and reduced by 43.4 % the hypotonic KCC activity (Fig. 7a, b). In accordance with these results, RVD was inhibited by the blockers. The effect was more evident at the first phase (300 s) of the volume regulatory process, when DIOA and DCPIB reduced by RVD by 25.4 and 34.4 %, respectively, and these effects were additive (Fig. 7c).

Regulatory volume increase

Cells exposed to a medium made hypertonic by addition of sorbitol to reach a final osmolarity of 600 mOsm (see "Materials and methods") initially shrink and immediately after, initiate the adaptive process of volume recovery, known as regulatory volume increase (RVI). Figure 8a shows RVI in WNK3+ and WNK3-KD cells as compared

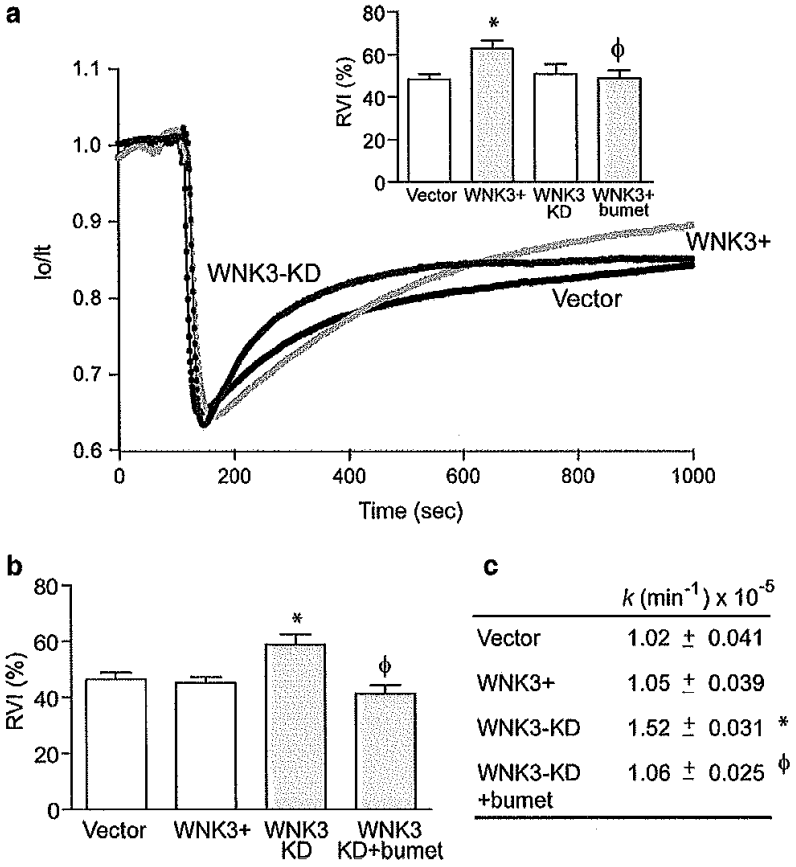

Fig. 8 Volume reduction and regulatory volume increase (RVI) after a hypertonic stimulus in control (V), WNK3+, or WNK3-KD cells. **a** Representative curves of changes in cell volume after hypertonic (600 mOsm) stimulus in each cell type. Cell shrinkage is followed by a biphasic process of RVI, with a first, fast component, evident at 110–300 s and a second slow component. *Bars* (*inset*) represent the cell volume recovery at the end of the experiment, calculated as percentage of maximal shrinkage. *Significantly different from RVI in control V cells at $P<0.05$; ϕ significantly different from WNK3+ without bumetanide at $P<0.05$. **b** RVI at the first component. **c** Rate constants from the slope calculated by fitting a linear regression to the logarithmically transformed data during the first 100 s after maximal shrinkage. *Significantly different from control V cells at $P<0.05$; ϕ significantly different from WNK3-KD without bumetanide at $P<0.05$. *Bars* (**a**, *inset*) represent the cell volume recovery at the end of the experiment, expressed as percentage of maximal swelling. **b** RVI calculated after the fast component of the volume recovery process. **c** Rate constants for the first RVI phase calculated as in Fig. 3c

to control V cells. The RVI pattern in control cells showed two phases of different rate, an initial, rapid phase lasting 110–300 s and a slow, second phase occurring up to 15 min. RVI efficiency at the end of the experiments in V cells was 48 % (Fig. 8a, b). Bumetanide decreased RVI only by 10.3± 2.4 % (results not shown). In WNK3+ cells, RVI was 30 % higher, due to a more rapid regulation at the second phase of the regulatory process (Fig. 8a, b). This effect was prevented by bumetanide (Fig. 8b). In WNK3-KD cells no difference was found in total RVI as compared to controls (Fig. 8a, b); however, these cells showed a significantly faster volume recovery at the initial phase, which was 26.2 % more rapid than in controls (Fig. 8a, c). This increased was abolished by bumetanide 10 μM (Fig 8a, c).

The effect of bumetanide preventing the increase in RVI in WNK3+ cells and the faster phase of the volume regulatory process in WNK-KD cells, suggest that the cotransporter NKCC is responsible for these differences. The activity of NKCC was then examined in controls and in the two experimental groups of cells, at the times corresponding to the two phases of RVI. Figure 9a shows that at short times (3 min) NKCC was not significantly increased by the hypertonic

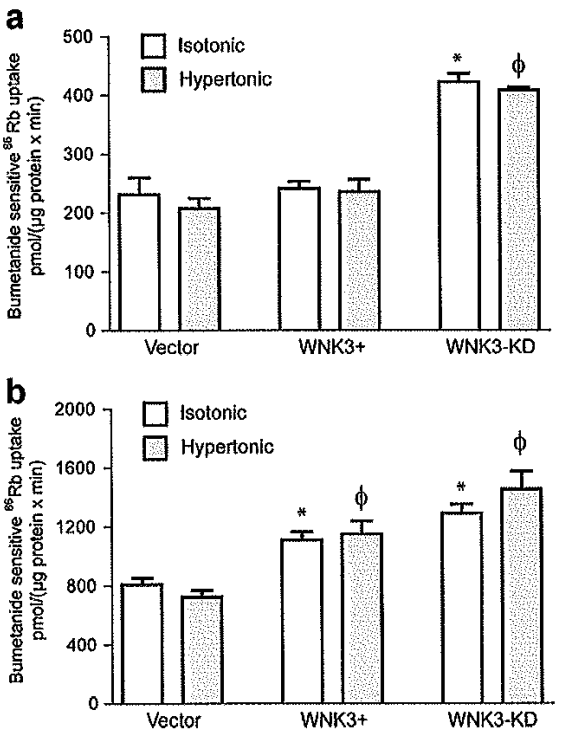

Fig. 9 NKCC activity in WNK3+ and WNK3-KD cells. Bumetanide-sensitive ^{86}Rb uptake assays were used to measure the NKCC activity, as described in "Materials and methods". **a** ^{86}Rb uptake at 3 min and **b** at 15 min. Experiments were performed in isotonic (*clear bar*) or hypertonic (*dark bar*) conditions. *Significantly different from isotonic control V cells at $P<0.05$; ϕ significantly different from control V cells in hypertonicity at $P<0.05$

condition in V cells, nor in WNK3+ cells, while in WNK3-KD cells, NKCC activity was markedly increased in isotonic conditions, and was not further enhanced by the hyperosmolar condition. This higher NKCC activity seems then responsible for the higher volume regulation in these cells at the fast initial phase shown in Fig. 8c. At longer times (15 min) NKCC activity in control cells was not increased by hypertonicity, but in WNK3+ or of WNK3-KD cells, NKCC activity significantly increased in isotonic conditions without further activity in hypertonic conditions (Fig. 9b). These results on the NKCC activity may explain the differences observed at the two phases of RVI in WNK3+ and WNK3-KD cells.

Discussion

In the present study in HEK293 cells, WNK3 was found localized at the intercellular junctions. This result confirms a report showing immunohistochemical expression of WNK3 at the cell junctions in a variety of epithelial tissue sections [17, 40]. The functional kinase is required for its localization at the cell junctions, since in cells with a mutated catalytic site, WNK3 is relocated and found predominantly at a perinuclear area, partly the trans-Golgi network (Fig. 2b, lower panel). The structures and mechanisms which determine the WNK3 intracellular localization are so far unclear. In terms of function, the presence of WNK3 at the intercellular junctions suggests a role in parallel Cl^- fluxes, as has been proposed for WNK1 or WNK4 [16, 30]. In contrast to HEK293 cells, in human glioma cells in culture, WNK3 is localized prominently at the cytosol, and associated with vacuole-like subcellular structures [12]. More information is necessary to define whether the intracellular localization of WNK3 is cell specific.

Introduction of a catalytic inactive WNK3 in HEK293 cells as in the present study induced a remarkable change in cell shape. This effect, not previously described, suggests an interaction of the active WNK3 with cell structures, possibly elements of the cytoskeleton, related to maintain the characteristic shape of these epithelial cells. A difference is found again with glioma cells, in which silencing of WNK3 by siRNA did not induce a change in cell shape [12].

In response to osmotic stimuli, WNK3 translocates to the cytosol (Fig. 2). This mobilization may be required to establish the interactions with signal molecules or structures related to cotransporter trafficking or/and for the cytoskeleton adaptations necessary to face the change in cell volume. No translocation of WNK3 into the cell membrane was observed, suggesting that its effects on the cotransporters occur via intermediate signaling chains ultimately responsible for the cotransporter activation. This chain most likely involves the Ste20-like kinases SPAK and OSR1, whose functional interaction with WNKs including WNK3 is well documented [33, 38].

The present results in HEK293 cells showed that WNK3 activity has a clear influence on RVD. The volume regulatory efficiency is reduced in cells overexpressing WNK3 (WNK3+) and markedly increased in cells expressing the catalytically inactive WNK3 (WNK3-KD cells). These effects are related to WNK3 effect on the cotransporter KCC (compare Figs. 3 and 6). It is known that the phosphorylation status of the KCC molecule determines the functional activity of the transporter, which is reduced by phosphorylation and increased by dephosphorylation [2, 18]. Dephosphorylation of two key phosphorylation sites, threonine residues 991 and 1048 of KCC3 have been clearly shown to be associated with activation of the cotransporter [40]. The present results in HEK293 cells demonstrate that the observations done in the heterologous expression system of *Xenopus* oocytes [5, 17] also occur in a mammalian cell system, confirming that WNK3 has a profound influence on the KCC activity, decreasing or increasing the cotransporter efficiency according to the presence or absence of catalytic

activity of the kinase. HEK293 cells under isotonic conditions express endogenous WNK3 and basal KCC activity, which are both suppressed in cells overexpressing WNK3. Conversely, in cells stably transfected with the kinase inactive by intervention of the catalytic site, the KCC activity increases dramatically. These results point to an effect of the WNK3 in the control of the phosphorylation state of the cotransporter, which involves the catalytic site of the kinase. This influence of WNK3 in isotonic conditions affects the KCC response to hypotonicity. In control cells, a mild decrease in osmolarity activates KCC, and this response is prevented in WNK3+ cells, suggesting that KCC is inactive by the overexpressed WNK3 and is unable to respond to hypotonicity. In WNK3-KD cells, containing the catalytically inactive WNK3, the KCC activity is already maximal and cannot be further increased by hypotonicity (Fig. 6). These results can be interpreted as to mean that inactivation of WNK3 promotes maximal dephosphorylation of the transporter molecules, which cannot be further increased by other stimuli. In experiments in oocytes expressing WNK3-KD, KCC activity also markedly increases in isotonic conditions, but in contrast to the present results in HEK293 cells, hypotonicity is still able to increase KCC activity over the level found in the isomolar condition [5, 17]. This may occur because in the oocyte study KCC is overexpressed, and thus cells may have a surplus of transporters to be activated by hypotonicity, not present in HEK293 cells. Disparities in the magnitude of the hypotonic stimulus, 50 % in oocytes and 15 % in HEK cells, may also explain this difference.

The present results, though clearly supporting the involvement of WNK3/KCC in RVD, showed that a substantial volume regulation is still found in WNK3+ cells in which KCC activity is almost abolished (Figs. 3 and 6), stress the important contribution of mechanisms for RVD other than the transporter, and independent of WNK3. The volume-sensitive Cl^- channel (Cl^-_{swell}) is a strong candidate, as a robust Cl^- current activates in control cells exposed to 15 % osmolarity reduction. This channel seems not to be under the influence of WNK3 since no significant difference was found in our study between control cells and WNK3+ or WNK3-KD cells. Potassium fluxes are also key contributors to RVD in most cells. Interestingly, K^+ translocation during RVD occurs not always via volume-sensitive K^+ channels but rather through a number of other K^+ channels activated by factors concurrent with hypotonicity and swelling. This is the case of voltage-sensitive channels, Ca^{2+}-dependent K^+ channels, or stretch-activated K^+ channels [14]. In fact, K^+ channels strictly dependent on swelling have described only in few cell types [28]. To our knowledge, the K^+ channel(s) involved in RVD in HEK293 cells have not been so far identified. Heterologous expression of TASK-2 in HEK-293 cells generates osmosensitive K^+ currents which contribute to volume regulation [27], but the TASK channels are not influenced by WNKs [18, 19]. WNK4 inhibits the maxi-K^+ channel heterologously expressed in HEK293 cells [48], but there is as yet no evidence of its contribution to RVD in these cells. WNK1, WNK3, and WNK4 inhibit the ROMK1 [20, 22, 24], but these channels are not involved in RVD [14]. Clarifying the role of WNKs on K^+ channels related to volume regulation is an interesting subject to be pursued in future investigations.

The relative contribution to RVD of the cotransporter and the volume-sensitive Cl^- channel could not be accurately measured in HEK293 cells since as here shown (Fig. 7), DIOA and DCPIB, considered as potent blockers of KCC and Cl^-_{swell}, respectively [6], interfere with both, the cotransporter and the channel activity. Also, the non-specific effect of DIOA, which inhibited the volume-sensitive K^+ fluxes has been previously reported [21]. These results should be taken into consideration when using these drugs as tools to evaluate the contribution of either one of these mechanisms to volume regulation [7, 44]. The contribution of KCC to RVD in HEK293 cells, where Cl^-_{swell} was unaffected by WNK3, may be evaluated by the differences in RVD efficiency found between WNK3+, WNK3-KD, in which KCC activity is either suppressed (WNK3+) or markedly increased (WNK3-KD).

The influence of WNK3 in the cell response to hypertonic conditions was examined in the present study. In HEK293 cells, hypertonic stimulus evoked a fast cell shrinkage followed by cell volume recovery. This adaptive process in most cells occurs by the operation of several mechanisms, i.e., channels, exchangers, and transporters. The present results suggest that in HEK293 cells the cotransporter NKCC is not prominently involved in RVI. This conclusion is based, first, in the low effect on RVI of the specific NKCC blocker bumetanide, and second, because NKCC was not activated by increases in external osmolarity in these cells ([15] and present results, Fig. 9). Although presumably not involved in RVI in physiological conditions, WNK3 showed a marked influence on NKCC activity in HEK293 cells. These cells have a low NKCC activity, but it can be many-fold increased by overexpression of WNK3. This is in accordance with previous results in oocytes [17]. NKCC activity in most cells depends on the phosphorylation status of the molecule and the WNK3 overexpression may increase the phosphorylated, active transporters [18]. Surprisingly, NKCC activity was also enhanced in cells expressing the inactive form of WNK3 (Fig. 9). We propose that this is due to the effect of the inactive kinase strongly increasing the activity of the KCC transporter, leading to a decrease in $[Cl^-]_i$ which is then, the stimulus increasing NKCC activity [11, 25]. Besides, the activity of endogenous WNK1 and WNK2, which are expressed in HEK293 cells [12], may contribute to the NKCC activity observed in the WNK3-KD cells. Thus, even though via different mechanisms, NKCC is activated in cells overexpressing either the active or the inactive form of WNK3, and

RVI was increased in the two cell lines. Altogether, these results show that even if NKCC is not a significant contributor to RVI in HEK293 cells, this process may be influenced by WNK3 due to its dual role affecting both KCC and NKCC, and through this effect, regulating the cell Cl^- levels. It is worthy to notice that steady state $[Cl^-]_i$ in control, WNK3+, and WNK3-KD cells was significantly different, with the following profile: WNK3+>control>WNK3-KD, due to the inhibition and activation of KCCs by wild-type WNK3 and catalytically inactive WNK3-KD, respectively. Even when this role of WNK3 regulating $[Cl^-]_i$ has been suggested [32], this is the first time, to our knowledge, that this has been demonstrated by direct evidence and using a mammalian cell system. Our data thus support the proposal that WNK3 could be the Cl^--sensitive kinase.

In contrast to HEK293 cells, RVI in glioma D54-MG cells is essentially dependent of NKCC, also under the influence of WNK3, since bumetanide at high concentrations, and silenced WNK3, abolished RVI in these cells [12]. Interestingly, WNK3 was not found expressed in normal glia [17] and there is essentially no information about the expression and activity of this kinase in other cell types.

WNK1 and WNK4 are also responsive to changes in external tonicity. WNK1 activates by hypertonicity and cell shrinkage and via the downstream signaling chain formed by the Ste20-kinases SPAK and OSR1, regulates the cotransporters NCC and NKCC, sustaining their functional activity [23, 43, 46, 47]. This sequence of events point to a role for WNK1 on the regulatory volume increase, although only few studies have effectively shown this action [4]. KCC3 is also subject of WNK1 influence, decreasing its activity upon phosphorylation. WNK1 also activates by hypotonicity though to a lower extent [23, 40]. WNK4 also regulates NCC, NKCC [3, 16], and KCCs ([8, 10], but its possible influence on volume regulation is so far unknown. A recent study in *X. laevis* oocytes revealed that WNK2, similar to WNK3, reciprocally activates NKCC1 and inactivates KCC2 in a kinase-dependent manner [41] Thus, it may also contribute to volume regulation in those cells where it is expressed.

In summary, the present study in HEK293 cells which documented the implication of WNK3 in cell volume control as well as in the regulation of intracellular Cl^- levels, contributes to support the influence on WNKs on these two important elements of cell homeostasis.

Acknowledgments We acknowledge the valuable technical assistance of Gabriel Orozco Hoyuela with the confocal microscopy. We thank Dra. Lorenza González-Mariscal for providing the antibody anti-occludin and Dr. Luis Vaca for providing the antibody anti-golgin-97. This work was supported by the Dirección General de Asuntos del Personal Académico (DGAPA), Universidad Nacional Autónoma de México (UNAM) [grant number IN203410 to H.P-M.], and Consejo Nacional de Ciencia y Tecnología (CONACyT) [grant number 98952 to H.P-M and 165815 to G.G.]. This work is part of the requirements for the Ph.D. degree in Biomedical Sciences of Silva Cruz-Rangel at UNAM, with a CONACyT fellowship.

References

1. Anselmo AN, Earnest S, Chen W, Juang YC, Kim SC, Zhao Y, Cobb MH (2006) WNK1 and OSR1 regulate the Na^+, K^+, $2Cl^-$ cotransporter in HeLa cells. Proc Natl Acad Sci U S A 103:10883–10888. doi:10.1073/pnas.0604607103
2. Bergeron MJ, Frenette-Cotton R, Carpentier GA, Simard MG, Caron L, Isenring P (2009) Phosphoregulation of K(+)–Cl(−) cotransporter 4 during changes in intracellular Cl(−) and cell volume. J Cell Physiol 219:787–796. doi:10.1002/jcp. 21725
3. Cai H, Cebotaru V, Wang YH, Zhang XM, Cebotaru L, Guggino SE, Guggino WB (2006) WNK4 kinase regulates surface expression of the human sodium chloride cotransporter in mammalian cells. Kidney Int 69:2162–2170. doi:10.1038/sj.ki.5000333
4. Choe KP, Strange K (2007) Evolutionarily conserved WNK and Ste20 kinases are essential for acute volume recovery and survival after hypertonic shrinkage in *Caenorhabditis elegans*. Am J Physiol Cell Physiol 293:C915–C927. doi:10.1152/ajpcell.00126.2007
5. de Los HP, Kahle KT, Rinehart J, Bobadilla NA, Vazquez N, San Cristobal P, Mount DB, Lifton RP, Hebert SC, Gamba G (2006) WNK3 bypasses the tonicity requirement for K–Cl cotransporter activation via a phosphatase-dependent pathway. Proc Natl Acad Sci U S A 103:1976–1981. doi:10.1073/pnas.0510947103
6. Decher N, Lang HJ, Nilius B, Brüggemann A, Busch AE, Steinmeyer K (2001) DCPIB is a novel selective blocker of I(Cl, swell) and prevents swelling-induced shortening of guinea-pig atrial action potential duration. Br J Pharmacol 134:1467–79. doi:10.1038/sj.bjp. 0704413
7. Ernest NJ, Weaver AK, Van Duyn LB, Sontheimer HW (2005) Relative contribution of chloride channels and transporters to regulatory volume decrease in human glioma cells. Am J Physiol Cell Physiol 288:C1451–C1460. doi:10.1152/ajpcell.00503.2004
8. Gagnon KB, England R, Delpire E (2006) Volume sensitivity of cation–Cl-cotransporters is modulated by the interaction of two kinases: Ste20-related proline-alanine-rich kinase and WNK4. Am J Physiol Cell Physiol 290:C134–142. doi:10.1152/ajpcell.00037.2005
9. Gamba G (2005) Molecular physiology and pathophysiology of electroneutral cation–chloride cotransporters. Physiol Rev 85:423–93. doi:10.1152/physrev.00011.2004
10. Garzon-Muvdi T, Pacheco-Alvarez D, Gagnon KB, Vazquez N, Ponce-Coria J, Moreno E, Delpire E, Gamba G (2007) WNK4 kinase is a negative regulator of K^+–Cl^- cotransporters. Am J Physiol Renal Physiol 292:F1197–F1207. doi:10.1152/ajprenal.00335.2006
11. Gillen CM, Forbush B III (1999) Functional interaction of the K–Cl cotransporter (KCC1) with the Na–K–Cl cotransporter in HEK-293 cells. Am J Physiol Cell Physiol 276:C328–C336
12. Haas BR, Cuddapah VA, Watkins S, Rohn KJ, Dy TE, Sontheimer H (2011) With-no-lysine kinase 3 (WNK3) stimulates glioma invasion by regulating cell volume. Am J Physiol Cell Physiol 301:C1150–C1160. doi:10.1152/ajpcell.00203.2011
13. Hayashi H, Suruga K, Yamashita Y (2009) Regulation of intestinal Cl^-/HCO_3^- exchanger SLC26A3 by intracellular pH. Am J Physiol Cell Physiol 296:C1279–C1290. doi:10.1152/ajpcell.00638.2008
14. Hoffmann EK, Pedersen SF (2011) Cell volume homeostatic mechanisms: effectors and signalling pathways. Acta Physiol 202:465–485. doi:10.1111/j.1748-1716.2010.02190.x
15. Isenring P, Jacoby SC, Payne JA, Forbush B 3rd (1998) Comparison of Na–K–Cl cotransporters. NKCC1, NKCC2, and the HEK cell Na–L–Cl cotransporter. J Biol Chem 273:11295–301. doi:10.1074/jbc.273.18.11295

16. Kahle KT, Gimenez I, Hassan H, Wilson FH, Wong RD, Forbush B, Aronson PS, Lifton RP (2004) WNK4 regulates apical and basolateral Cl^- flux in extrarenal epithelia. Proc Natl Acad Sci U S A 101:2064–2069. doi:10.1073/pnas.0308434100
17. Kahle KT, Rinehart J, de Los HP, Louvi A, Meade P, Vazquez N, Hebert SC, Gamba G, Gimenez I, Lifton RP (2005) WNK3 modulates transport of Cl^- in and out of cells: implications for control of cell volume and neuronal excitability. Proc Natl Acad Sci U S A 102:16783–16788. doi:10.1073/pnas.0508307102
18. Kahle KT, Rinehart J, Lifton RP (2010) Phosphoregulation of the Na–K–2Cl and K–Cl cotransporters by the WNK kinases. Biochim Biophys Acta 1802:1150–1158. doi:10.1016/j.bbadis.2010.07.009
19. Kahle KT, Ring AM, Lifton RP (2008) Molecular physiology of the WNK kinases. Annu Rev Physiol 70:329–355. doi:10.1146/annurev.physiol.70.113006.100651
20. Kahle KT, Wilson FH, Leng Q, Lalioti MD, O'Connell AD, Dong K, Rapson AK, MacGregor GG, Giebisch G, Hebert SC, Lifton RP (2003) WNK4 regulates the balance between renal NaCl reabsorption and K^+ secretion. Nat Genet 35:372–376. doi:10.1038/ng1271
21. Lauf PK, Misri S, Chimote AA, Adragna NC (2008) Apparent intermediate K conductance channel hyposmotic activation in human lens epithelial cells. Am J Physiol Cell Physiol 294:C820–C832. doi:10.1152/ajpcell.00375.2007
22. Lazrak A, Liu Z, Huang CL (2006) Antagonistic regulation of ROMK by long and kidney-specific WNK1 isoforms. Proc Natl Acad Sci U S A 103:1615–1620. doi:10.1073/pnas.0510609103
23. Lenertz LY, Lee BH, Min X, Xu BE, Wedin K, Earnest S, Goldsmith EJ, Cobb MH (2005) Properties of WNK1 and implications for other family members. J Biol Chem 280:26653–26658. doi:10.1074/jbc.M502598200
24. Leng Q, Kahle KT, Rinehart J, MacGregor GG, Wilson FH, Canessa CM, Lifton RP, Hebert SC (2006) WNK3, a kinase related to genes mutated in hereditary hypertension with hyperkalaemia, regulates the K^+ channel ROMK1 (Kir1.1). J Physiol 571:275–286. doi:10.1113/jphysiol.2005.102202
25. Lytle C, McManus T (2002) Coordinate modulation of Na–K–2Cl cotransport and K–Cl cotransport by cell volume and chloride. Am J Physiol Cell Physiol 283:C1422–C1431. doi:10.1152/ajpcell.00130.2002
26. McCormick JA, Ellison DH (2011) The WNKs: atypical protein kinases with pleiotropic actions. Physiol Rev 91:177–219. doi:10.1152/physrev.00017.2010
27. Niemeyer MI, Cid LP, Barros LF, Sepúlveda FV (2001) Modulation of the two-pore domain acid-sensitive K^+ channel TASK-2 (KCNK5) by changes in cell volume. J Biol Chem 276:43166–43174. doi:10.1074/jbc.M107192200
28. Niemeyer MI, Hougaard C, Hoffmann EK, Jorgensen F, Stutzin A, Sepúlveda FV (2000) Characterisation of a cell swelling-activated K^+-selective conductance of Ehrlich mouse ascites tumour cells. J Physiol 524:757–767. doi:10.1111/j.1469-7793.2000.00757.x
29. Nilius B, Eggermont J, Voets T, Buyse G, Manolopoulos V, Droogmans G (1997) Properties of volume-regulated anion channels in mammalian cells. Prog Biophys Mol Biol 68:69–119. doi:10.1016/S0079-6107(97)00021-7
30. Ohta A, Yang SS, Rai T, Chiga M, Sasaki S, Uchida S (2006) Overexpression of human WNK1 increases paracellular chloride permeability and phosphorylation of claudin-4 in MDCKII cells. Biochem Biophys Res Commun 349:804–808. doi:10.1016/j.bbrc.2006.08.101
31. Okada Y (2004) Ion channels and transporters involved in cell volume regulation and sensor mechanisms. Cell Biochem Biophys 41:233–258. doi:10.1385/CBB:41:2:233
32. Pacheco-Alvarez D, Gamba (2011) WNK3 is a putative chloride sensitive kinase. Cell Physiol Biochem 28:1123–1134. doi:10.1159/000335848
33. Pacheco-Alvarez D, Vázquez N, Castañeda-Bueno M, de-Los-Heros P, Cortes-González C, Moreno E, Meade P, Bobadilla NA, Gamba G (2012) WNK3-SPAK interaction is required for the modulation of NCC and other members of the SLC12 family. Cell Physiol Biochem 29:291–302. doi:10.1159/000337610
34. Pasantes-Morales H (2007) Amino acids and brain volume regulation. In: Oja S, Schousboe A, Saraansari P (eds) Handbook of neurochemistry and molecular neurobiology, 3rd edn. Springer, New York, pp 225–248
35. Pasantes-Morales H, Cruz-Rangel S (2010) Brain volume regulation: osmolytes and aquaporin perspectives. Neuroscience 168:871–84. doi:10.1016/j.neuroscience.2009.11.074
36. Pedersen SF, Beisner KH, Hougaard C, Willumsen BM, Lambert IH, Hoffmann EK (2002) Rho family GTP binding proteins are involved in the regulatory volume decrease process in NIH3T3 mouse fibroblasts. J Physiol 541:779–796. doi:10.1113/jphysiol.2002.018887
37. Ponce-Coria J, San-Cristobal P, Kahle KT, Vazquez N, Pacheco-Alvarez D, de Los Heros P, Juarez P, Munoz E, Michel G, Bobadilla NA, Gimenez I, Lifton RP, Hebert SC, Gamba G (2008) Regulation of NKCC2 by a chloride-sensing mechanism involving the WNK3 and SPAK kinases. Proc Natl Acad Sci U S A 105:8458–8463. doi:10.1073/pnas.0802966105
38. Richardson C, Alessi DR (2008) The regulation of salt transport and blood pressure by the WNK-SPAK/OSR1 signalling pathway. J Cell Sci 121:3293–304. doi:10.1242/jcs.029223
39. Rinehart J, Kahle KT, de Los Heros P, Vazquez N, Meade P, Wilson FH, Hebert SC, Gimenez I, Gamba G, Lifton RP (2005) WNK3 kinase is a positive regulator of NKCC2 and NCC, renal cation–Cl cotransporters required for normal blood pressure homeostasis. Proc Natl Acad Sci U S A 102:16777–16782. doi:10.1073/pnas.0508303102
40. Rinehart J, Maksimova YD, Tanis JE, Stone KL, Hodson CA, Zhang J, Risinger M, Pan W, Wu D, Colangelo CM, Forbush B, Joiner CH, Gulcicek EE, Gallagher PG, Lifton RP (2009) Sites of regulated phosphorylation that control K–Cl cotransporter activity. Cell 138:525–536. doi:10.1016/j.cell.2009.05.031
41. Rinehart J, Vázquez N, Kahle KT, Hodson CA, Ring AM, Gulcicek EE, Louvi A, Bobadilla NA, Gamba G, Lifton RP (2011) WNK2 kinase is a novel regulator of essential neuronal cation-chloride cotransporters. J Biol Chem 286:30171–30180. doi:10.1074/jbc.M111.222893
42. Russell JM (2000) Sodium–potassium–chloride cotransport. Physiol Rev 80:211–276
43. Shaharabany M, Holtzman EJ, Mayan H, Hirschberg K, Seger R, Farfel Z (2008) Distinct pathways for the involvement of WNK4 in the signaling of hypertonicity and EGF. FEBS J 275:1631–1642. doi:10.1111/j.1742-4658.2008.06318.x
44. Taouil K, Hannaert P (1999) Evidence for the involvement of K^+ channels and K(+)–Cl^- cotransport in the regulatory volume decrease of newborn rat cardiomyocytes. Pflugers Arch 439:56–66. doi:10.1007/s004240051128
45. Vázquez-Juárez E, Ramos-Mandujano G, Lezama RA, Cruz-Rangel S, Islas LD, Pasantes-Morales H (2008) Thrombin increases hyposmotic taurine efflux and accelerates ICI-swell and RVD in 3 T3 fibroblasts by a src-dependent EGFR transactivation. Pflugers Arch 455:859–872. doi:10.1007/s00424-007-0343-y
46. Xu B, English JM, Wilsbacher JL, Stippec S, Goldsmith EJ, Cobb MH (2000) WNK1, a novel mammalian serine/threonine protein kinase lacking the catalytic lysine in subdomain II. J Biol Chem 275:16795–16801. doi:10.1074/jbc.275.22.16795
47. Zagorska A, Pozo-Guisado E, Boudeau J, Vitari AC, Rafiqi FH, Thastrup J, Deak M, Campbell DG, Morrice NA, Prescott AR, Alessi DR (2007) Regulation of activity and localization of the WNK1 protein kinase by hypertonic stress. J Cell Biol 176:89–100. doi:10.1083/jcb.200605093
48. Zhuang J, Zhang X, Wang D, Li J, Zhou B, Shi Z, Gu D, Denson DD, Eaton DC, Cai H (2011) WNK4 kinase inhibits Maxi K channel activity by a kinase-dependent mechanism. Am J Physiol Renal Physiol 301:F410–F419. doi:10.1152/ajprenal.00518.2010